Two-photon fluorescence lifetime imaging monitors metabolic changes during wound healing of corneal epithelial cells in vitro

Uta Gehlsen[1,2A;D], Andrea Oetke[1A], Marta Szaszák[3A], Norbert Koop[4A], Friedrich Paulsen[B], Andreas Gebert[C], Gereon Huettmann[4A], Philipp Steven[1,2A;D]

[1] Department of Ophthalmology, [2] Institute of Anatomy, [3] Institute of Medical Microbiology and Hygiene,
[4] Institute of Biomedical Optics, [5] Institute of Medical Biometry and Statistics
[A] University of Luebeck, Germany
[B] Institute of Anatomy and Cell Biology, University of Erlangen, Germany
[C] Institute of Anatomy II, University of Jena, Germany
[D] Department of Ophthalmology, University Clinic of Cologne, Germany

Corresponding author: Philipp Steven, MD, Department of Ophthalmology, University Clinic of Cologne, Kerpenerstr. 62, 50937 Cologne, Germany, Phone: +49-221 478-97790; Fax: +49-221 478-97836; Email: philipp.steven@uk-koeln.de

The authors have full control of the primary data and agree to allow Graefes Archive for Clinical and Experimental Ophthalmology to review the data on request.

Abstract

Background:
Early and correct diagnosis of delayed or absent corneal epithelial wound healing is a key factor to prevent infection and consecutive destruction of the corneal stroma with impending irreversible visual loss. Two-photon microscopy (TPM) is a novel technology that has potential to depict epithelial cells and to evaluate cellular function by measuring autofluorescence properties such as fluorescence intensity and fluorescence lifetimes of metabolic co-factors such as NAD(P)H.
Methods:
Using non invasive TPM in a tissue culture scratch model and an organ culture erosion model, fluorescence intensity and fluorescence lifetimes of NAD(P)H were measured before and during closure of the epithelial wounds. Influence of temperature and selective inhibition of metabolism on intensity and lifetimes were tested additionally.
Results:
Decrease of temperature resulted in significant decrease of fluorescence lifetimes and increase of the relative amount of free NAD(P)H due to decreased global metabolism. Increase in temperature and upregulation of glycolysis through blocking the mitochondrial electron transport chain by rotenone resulted in increased intensity, decreased lifetimes and increase in the relative amount of free NAD(P)H. Changes of lifetimes and free:protein-bound NAD(P)H ratios were similar to changes measured during wound healing in both scratch and erosion models.
Conclusions:
Fluorescence lifetime measurements (FLIM) detected enhancement of cellular metabolism following epithelial damage in both models. The prospective detection of cellular autofluorescence *in vivo*, in particular FLIM of metabolic cofactor NAD(P)H, has the potential to become an inevitable tool in clinical use to differentiate healing from non-healing epithelial cells and to evaluate effects of newly developed substances on cellular metabolism in preclinical and clinical trials.

Introduction

Early and correct diagnosis of delayed or absent corneal epithelial wound healing is a key factor to prevent infection and consecutive destruction of the corneal stroma with impending irreversible visual loss. Due to the complexity of underlying diseases such as neurotrophic keratitis, Stevens-Johnson syndrome or graft-vs.-host disease with extensive or complete loss of epithelial limbal stem cells this is often demanding and difficult [1-4]. Imaging techniques are available to support the clinician evaluating the patient's situation. The generally available technique is the use of slit-lamp microscopy together with staining of the ocular surface by fluorescing stains. The physician then evaluates the character and size of the defect. Optical coherence tomography (OCT) or confocal laser scanning microscopy (CLSM) are other well established techniques that are able to depict epithelial defects non-invasively and repeatedly and help the physician to estimate epithelial defects in addition to slit-lamp investigations [5, 6]. However neither CLSM nor OCT is able to collect information related to cellular function due to the imaging modalities that are solely based on reflectance microscopy.
Compared to CLSM and OCT non-invasive two-photon microscopy (TPM) is a promising technology readily used in ocular surface research but not yet established for imaging of the living human eye. TPM enables imaging of ocular tissues by using different excitation wavelengths and emission detectors and hereby gathers more structural information than CLSM or OCT [7-9]. Furthermore it has the potential to detect fluorescent metabolites *in vivo*. This non-invasive detection of metabolic cofactors such as reduced adenine dinucleotide (NAD(P)H) and flavin adenine dinucleotide (FAD) allows cutting-edge functional imaging that has already been used to monitor changes in cellular metabolism in human breast cells, macrophages, cardiomyocytes, corneal keratocytes and bacteria-infected cells [10-17]. NAD(P)H and FAD feature strong autofluorescence in contrast to the oxidized NAD^+ and reduced $FAD(H)_2$ that do not or just minimal elicit fluorescence. NAD(P)H and FAD^+ feature distinct fluorescence excitation (*Exc*) and emission (*Em*) maxima (FAD^+ *Exc*: around 900nm ; *Em*: 535nm and NAD(P)H: *Exc*: below 800nm ; *Em*: 450nm) [18]. By using selected excitation and fluorescence wavelengths NAD(P)H or FAD^+ may therefore be imaged and analyzed selectively.
TPM-excited fluorescence can be analyzed by its intensity and lifetime. Fluorescence intensity hereby depends on the concentration of intrinsic fluorophores and is also sensitive to photobleaching. Because of this, appropriate quantitative analyses and translation of fluorescence intensity into concentration values are difficult and subject to strong variations [19]. In contrast fluorescence lifetime imaging (FLIM) is a method to characterize metabolism independent of a given concentration of fluorophores. A fluorescence lifetime is the average time a molecule stays in its excited state before emitting a photon. It is therefore independent of its local concentration, but strongly depends on the protein binding and microenvironment of the molecules [20]. This makes FLIM highly interesting for analyzing cellular metabolism using non invasive TPM. As cellular metabolism is directly related to wound healing processes, a change of metabolic cofactors within the cellular microenvironment of corneal epithelial cells following injury should enable to differentiate these cells from non-injured cells. In this context NAD(P)H is the most important cofactor during cellular metabolism and

its concentration and protein binding should therefore be related to changes in metabolism during wound healing.
We hypothesized that the use of non invasive two-photon microscopy to excite and detect fluorescence, in particular fluorescence lifetimes of the metabolic cofactor NAD(P)H enables to monitor corneal epithelial wound healing following epithelial injury.

Materials and Methods

When wounded or scratched, cell monolayers respond by immediate migration of the cells. They polarize towards the wound, migrate and the monolayer closes. This is accompanied by varying degrees of cellular proliferation depending on the size of the wound. Instead, damaged cellular multilayers are repaired in several phases. An initial phase is characterized by extensive cellular organization at the wound edges and an absence of wound closure. This is followed by wound closure through horizontal migration of epithelial cells into the wound to form a basal monolayer. Finally these cells differentiate vertically into their appropriate layers [21-23]. In this study a monolayer and a multilayer model were used to test our hypothesis.

Cell culture and scratch model:

Human corneal epithelial cells (HCE-T cell line, RCB 2280) were cultured under standard tissue culture conditions (37° C, 5 % CO_2-atmosphere, Ham´s F12:MEM - 1:1). Medium was supplemented with Insulin (5µg/ml), Cholera toxin (1mg/ml), EGF (10ng/ml), Penicillin (100IU/ml)/Streptomycin (100µg/ml) and FBS (5%). 100.000 cells/dish were plated in 50 mm dishes on cover glasses two days prior measurements. The culture medium was HEPES buffered to achieve short term independency from CO_2 atmosphere and presumed pH changes during TPM. For TPM measurements, dishes were transferred to a custom made heated dish-holder that maintained 37° C (Fig. 1).

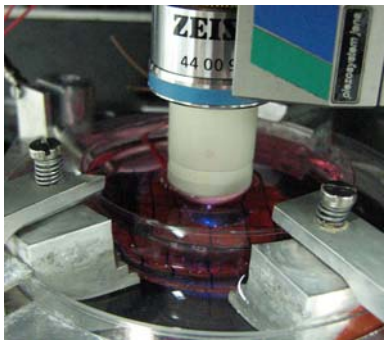

Figure 1: Custom made heated dish-holder

To test the setup, adding 10µM Rotenone to inhibit the ATP synthesis and to block the mitochondrial NADH oxidation two hours prior the measurements generated changes in cellular metabolism. To determine the dependence of cellular metabolism on the temperature, measurements were conducted at 20° C and 42° C. 10 individual two-photon measurements were done in every experimental set up. Individual controls were used because slight variations in confluence that may occur despite using standardized tissue culture conditions and defined numbers of plated cells are able to affect intensity and lifetime measurements [15].

To analyze cellular metabolism during epithelial wound healing, uniform scratches in HCE cell monolayers were generated mechanically to simulate trauma of the superficial corneal epithelial layer (Fig. 2a). Light microscopy demonstrated closure of the scratch within approximately 3 hours (Fig. 2b-d).

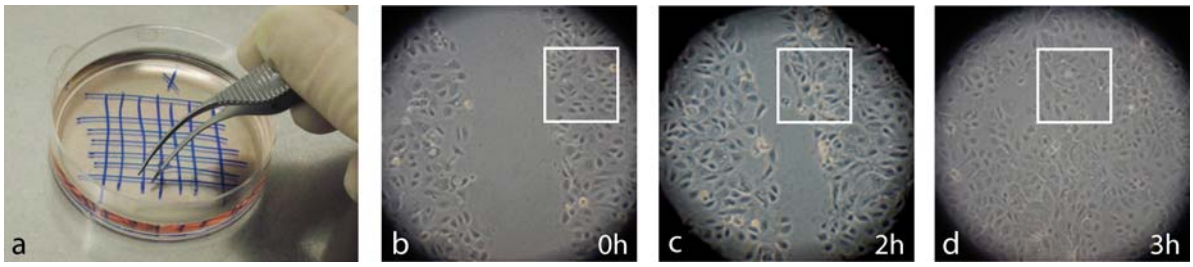

Fig. 2: Tissue culture scratch model (HCE-T cell line)
a: Scratches are generated using sterile forceps.
b-d: Within 3 hours post injury HCE-T cells close the scratch. The square depicts the area at the edge of the scratch measured by TPM.

Organ culture and erosion model:
An organ culture of explanted murine eyes was setup as reported previously [9]. Briefly female BALB/c mice, 12 weeks of age, were euthanized and eyes were removed with forceps without touching the epithelium. Explanted eyes were placed in petri dishes and fixed with tissue glue (VetBond, 3M Deutschland GmbH, Neuss, Germany). Erosions were caused by topical application of 0.5% NaOH to the central enucleated eyes for 2 minutes using a Whatman filter paper (Fig. 3a). The enucleated eyes were covered with prewarmed culture medium (DMEM F12, Sigma-Aldrich, Munich, Germany). To display the time course of wound healing in the explanted murine eye model an 830 nm spectral domain optical-coherence tomograph (Callisto, Thorlabs GmbH, Munich, Germany) was used. Three-dimensional scans (600 x 600 A-scans; Range: x=3.5mm, y=3.5mm) were performed every 8 hours until closure of the erosion. Eyes were transferred back to incubator between measurements and medium was changed.

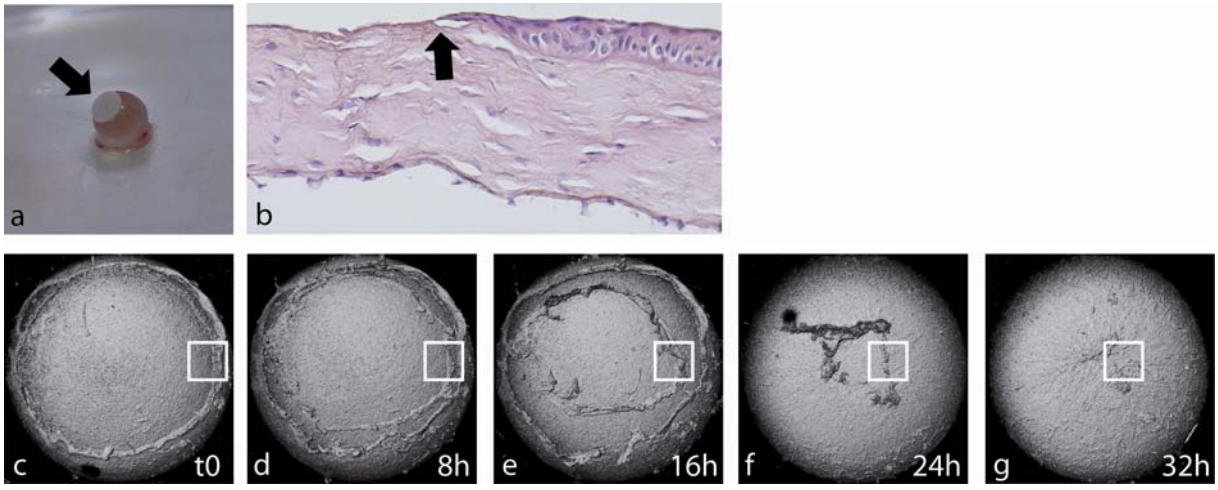

Figure 3: Explanted murine eye model
a: Explanted eye with a NaOH-containing filter paper (arrow) placed on the cornea. b: Section through the edge of the erosion. At the leading edge epithelial cells are elongated (arrow) and stretch towards the central cornea.
c-g: OCT imaging of the cornea demonstrates the time course of epithelial wound healing until closure of the erosion over 32 hours. The square depicts the area of interest for TPM at the leading edge of the epithelium.

Two-photon microscope:
A modified two-photon microscope (DermaInspect, Jenlab, Germany) equipped with a solid-state, tunable Ti:sapphire IR femtosecond laser (MaiTai, Spectra Physics, Germany, tuning range 710nm-920nm) and a 40x/0.8w lR-Achroplan objective (Zeiss, Germany) was used. The scan area was 107µm x 107µm.
FLIM data were collected by a single-photon counting(TPSPC) system with dedicated detector (PMH-100-0) and electronics (SPC-830, both Becker&Hickl, Berlin, Germany).

Two-photon measurements
Fluorescence intensity and fluorescence lifetime imaging (FLIM) were conducted under standardized conditions (730 nm excitation wavelength, 20 mW laser energy, 36° C, acquisition time 49 seconds) at different time points during the closure of the scratch/erosion (Tab.1). 10 individual cell cultures (5 scratch, 5 controls) and 10 individual explanted eyes (5 erosion, 5 controls) were measured, conducting five measurements at each time point. All measurements in the treatment groups were performed at the leading edge of the scratch or erosion.

Time Point	Scratch + Controls	Erosion + Controls
t-1	before scratch	1 hour before erosion
t0	immediately after scratch	immediately after erosion
t1	30 minutes after scratch	8 hours after erosion
t2	60 minutes after scratch	16 hours after erosion
t3	90 minutes after scratch	24 hours after erosion
t4	120 minutes after scratch	32 hours after erosion
t5	-	40 hours after erosion

Tab. 1: Measurement time points

Data analysis:
The lifetime decay curve was fitted to a double exponential decay by SPCImage software (Version 2.9.8., Becker & Hickl, Germany). Instrument response function was measured from second harmonic generation signal of beta-barium-borate crystal.
For determining fluorescence intensities, photon counts in regions-of-interest were exported from ImageJ [24] to Excel software (Microsoft, Redmond, USA).

Statistical analysis:

Statistical analysis included Kruskal-Wallis Test and Mann-Whitney U-Test. Kruskal-Wallis Test was used to test data sets for different distribution. For further analysis Mann-Whitney U-Test was used to test data from controls vs. treatment groups for each time point. Data sets were analyzed with SPSS software (19.0 and 20.0, IBM, USA). As statistical analysis and interpretation were conducted for each individual experiment p-values <0.05 were considered to be significant.

Results

Autofluorescence intensity changes in HCE cells following inhibition of metabolism

In eukaryotic cells, the majority of cellular autofluorescence originates from the metabolic coenzyme NAD(P)H. Thus the autofluorescence intensity is positively correlated to the concentration of the fluorophores. We studied the effect of changing the cellular microenvironment by altering temperature and the effect of inhibition of NAD(P)H-binding enzymes on autofluorescence intensity in HCE cells. Incubation of HCE cells at 20° C decreased cellular autofluorescence intensity, while 42° C had no effect compared to 36° C (Fig. 4a). Using specific inhibitor of the mitochondrial electron transport chain we found that the complex I inhibitor, rotenone significantly increased autofluorescence intensity (Fig. 4b)

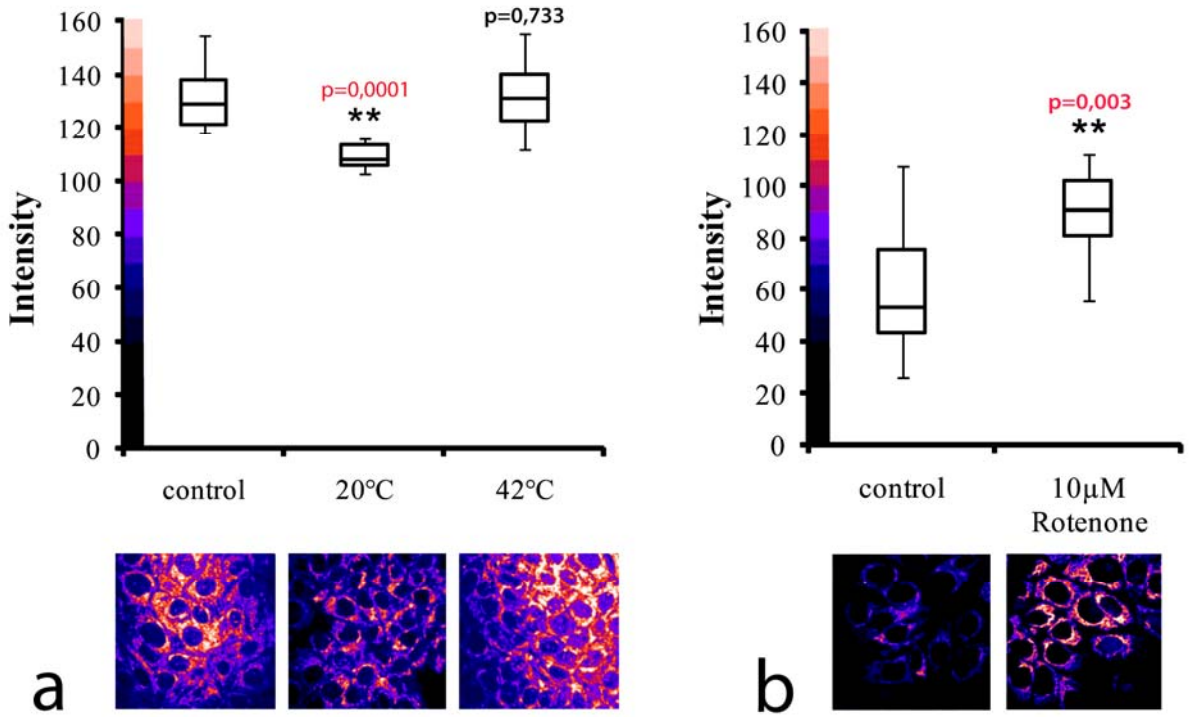

Fig. 4: Fluorescence intensity measurements of HCE-T tissue culture *in vitro*.
a: False colour images show change of the autofluorescence intensity in comparison to control (36° C, untreated culture). Decrease of temperature causes significant lowering of intensity by decreasing of cytoplasmic and mitochondrial metabolism in general.
b: Blocking mitochondrial NAD(P)H oxidation by rotenone increases fluorescence intensity. Intensity images are colour coded according to the scale bar within the figure. (Median ± SD, n=10, Kruskal-Wallis Test: p=0.0001, Mann-Whitney U-Test: p-values see figure)

Fluorescence lifetime changes are sensitive indicators of metabolic changes in HCE cells.

Fluorescence lifetime depends on microenvironment and protein-binding but is independent of the concentrations of the fluorophore. Therefore, we tested the effect of temperature and

metabolic inhibitors on fluorescence lifetimes. The fluorescence lifetime was fitted to a two component exponential decay (a1 Exp (t/t1) + a2 Exp (t/t2)) indicating a contribution of a short and a long fluorescence lifetime components. The median NAD(P)H-related fluorescence lifetime (tm) was 1200-1250ps while the short lifetime component (t1, free NAD(P)H) was appr. 260ps and the long lifetime was appr. 2250ps (t2, protein-bound NAD(P)H). The ratio of the contributions of short and long lifetimes (a1/a2) was 6.1±0.19/6.0±0.2 in non-treated control HCE cells respectively. Both temperature changes and application of rotenone caused significant changes in tm and a1/a2, which is attributed to the ratio of free to protein-bound NAD(P)H fluorescence. (Fig.5). At 20° C tm increased to appr. 1500ps whereas at 42° C tm decreased to appr. 980ps. Rotenone also decreased overall lifetime to appr. 960ps.

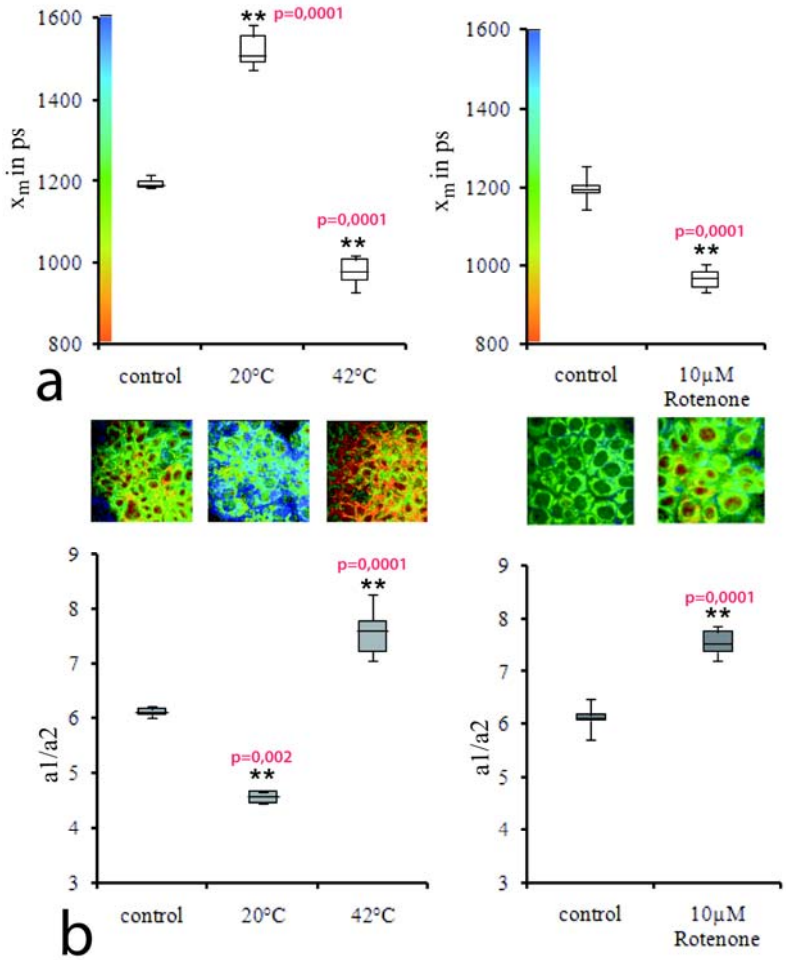

Fig. 5: Fluorescence lifetime imaging (FLIM) of HCE-T tissue culture *in vitro*.
a: Average fluorescence lifetimes (tm) are related to experiments shown in Fig. 4. Temperature reduction increased tm, whereas temperature increase had an opposite effect. Rotenone decreased lifetimes.
b: Ratio of short and long lifetime amplitudes (a1/a2) are decreased at 20° C and increased at 42° C. Rotenone increased a1/a2.
Representative FLIM-images are colour coded according to the scale bar. (Median ± SD, n=10, Kruskal-Wallis Test: p=0.0001, Mann-Whitney U-Test: p-values see figure)

Autofluorescence intensity detection in cell culture scratch model

Quantitative analysis of autofluorescence in the cell culture scratch model demonstrated a slight increase of intensity over the measurement period of 120 minutes, whereas fluorescence intensity in the control cell cultures decreased over time. However differences between scratch and control groups were statistically not significant (Fig. 6).

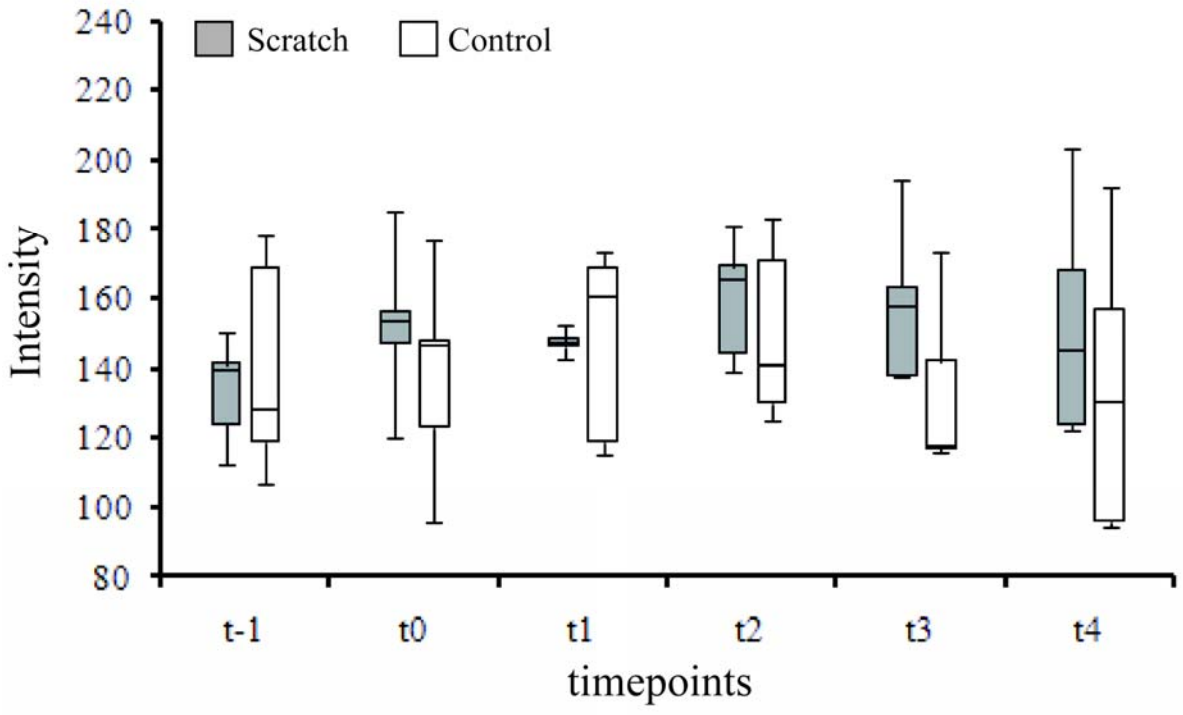

Fig.6: Fluorescence intensity measurements in HCE tissue culture scratch model. Autofluorescence intensities were quantitatively analyzed at 30min intervals. Autofluorescence intensity values of scratch cultures (grey boxes) non scratched control culture (white boxes) were not statistically different. (Median ± SD n= 5; Kruskal Wallis-Test: p=0.918)

FLIM in cell culture scratch model

At t-1 median fluorescence lifetime (tm) was appr. 1330ps in the scratch and the control group (Fig. 7). After injury (t0) tm decreased to values around 1270ps. This was followed by a slow increase towards 1340ps at t1. tm remained stable at this level until t4. The control values increased steadily until 1440ps at t2 and decreased slightly to 1420ps at t4. Differences between scratch control groups were all significant at t0 and after.
Calculation of free:protein-bound NAD(P)H ratio (a1/a2) demonstrated equal values at t-1 for both scratch group and controls. a1/a2 ratio increased to 6.5 at t0 followed by a decrease to 6.1 at t1. Values then remained stable until t4. In the controls values constantly decreased from t-1 to t4 and were significant lower than the values from the scratch group (Fig. 7).

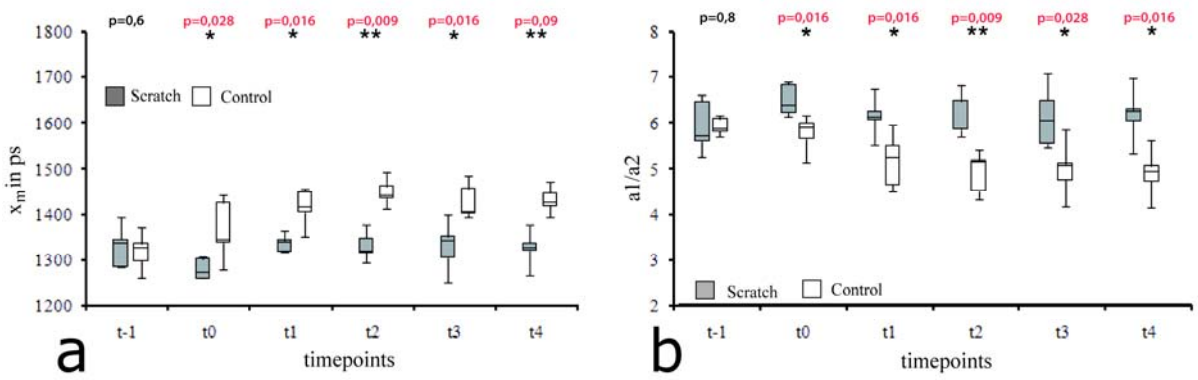

Fig. 7: Fluorescence lifetime in HCE tissue culture scratch model.
a: Control cultures (white boxes) show an increase in tm over time. Scratch cultures (grey boxes) show a significant decrease in tm after scratch compared to control.
(Median ± SD, n= 5; Kruskal Wallis-Test: p=0.001, Mann-Whitney U-Test: p-values see figure)
b: Control cultures (white boxes) demonstrate a decrease in free:protein-bound NAD(P)H ratio (a1/a2), whereas the scratch culture (grey boxes) show a significant higher free: protein NAD(P)H ratio than the control.
(Kruskal Wallis-Test: p=0.00005, Mann-Whitney U-Test: p-values see figure)

<u>Autofluorescence intensity detection in organ culture erosion model</u>
Quantitative analysis of autofluorescence intensity in the organ culture erosion model demonstrated a decrease in both erosion and control groups. Differences between the groups were statistically not significant (Fig. 8).

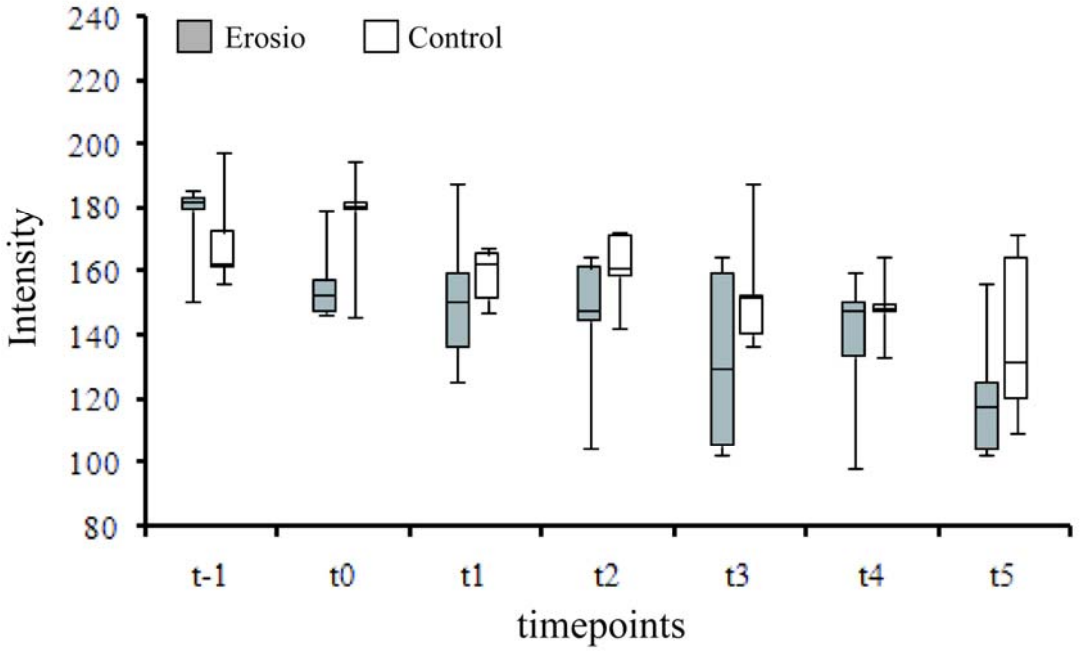

Fig. 8: Fluorescence intensity measurements in organ culture erosion model. Autofluorescence intensities were quantitatively analyzed at 8 hourly intervals. Autofluorescence intensity values of erosion cultures (grey boxes) and control cultures (white boxes) were not statistically different. (Median ± SD n= 5; Kruskal Wallis-Test: p=0.013)

FLIM in organ culture erosion model

Before erosion median fluorescence lifetime (tm) was appr. 1380ps in both experimental groups. Following erosion tm decreased to 1330ps and then steadily increased to a maximum of appr. 1520ps at t4. The control group demonstrated an increase of fluorescence lifetimes until t1, followed by a slight decrease until t3 and a final increase to a maximum of 1600ps at t5. Except at t3 all fluorescence lifetime measurements post-injury were significant lower in the erosion group (Fig. 9a). Calculating free:protein-bound NAD(P)H ratios (a1/a2) demonstrated significant differences between the two experimental groups at all time points post injury. a1/a2 ratio increased in the erosion group at t0 and decreased until below 4 at t5. In the controls a1/a2 ratio decreased from t-1 until t1, increased slightly from t1 to t3 and decrease to a minimum of 3.2 at t5 (Fig. 9b)

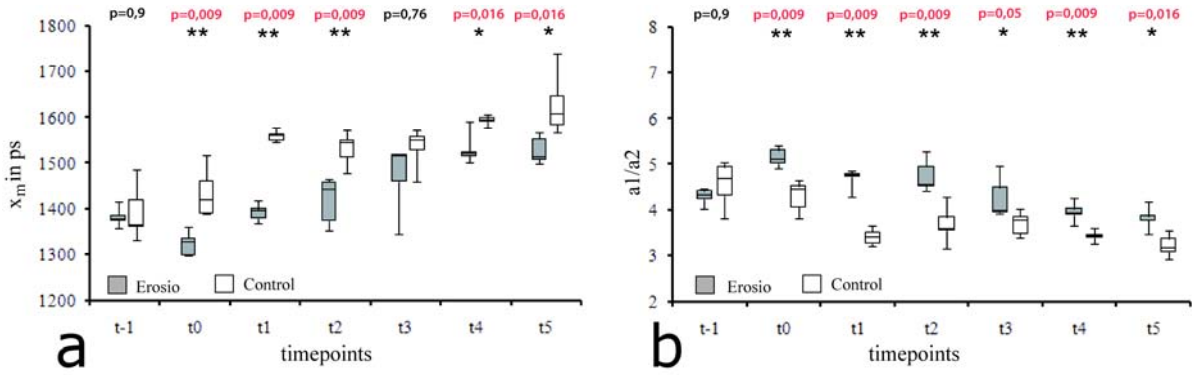

Fig. 9: Fluorescence lifetimes of organ culture erosion model. Fluorescence lifetime and free:protein-bound NAD(P)H ratio (a1/a2) were quantitatively analyzed at 8 hourly intervals.
a: Fluorescence lifetimes in the erosion group (grey boxes) are significantly shorter compared to control eyes (white boxes), except at t3.
(Median ± SD, n= 5, Kruskal Wallis-Test: p=0.025, Mann-Whitney U-Test: p-values see figure)
b: Erosion group (grey boxes) has a significant higher a1/a2 ratio than control eyes (white boxes).
(Median ± SD, n= 5, Kruskal Wallis-Test: p=0.004, Mann-Whitney U-Test: p-values see figure)

Discussion

Early and precise clinical detection and assessment of dysfunctional corneal epithelial wound healing is important to prevent corneal damage due to delays in appropriate therapy or misinterpretation of the clinical situation. This requires a suitable imaging technique that allows measuring epithelial function on a cellular level, ideally without the necessity of tissue probing. In contrast to established imaging techniques such as CLSM and OCT, two-photon microscopy (TPM) has been demonstrated to provide detailed structural information of the cornea based on tissue autofluorescence and second harmonic generation (SHG) [4]. In addition our group has previously demonstrated that non-invasive TPM is superior to CLSM to characterize pathologies of the ocular surface by detecting autofluorescence intensities and measuring fluorescence lifetimes [8]. Besides fluorescence intensity detection, fluorescence lifetime imaging (FLIM) is suitable to differentiate excited fluorophores in further detail and independent of the concentration of the fluorophores. The by far most relevant intrinsic fluorophore in TPM is NAD(P)H, as this molecule is present at different concentrations in all cellular compartments including mitochondria, cytosol and nucleus and features strong autofluorescence properties at excitation wavelengths of 710-750nm. In terms of wound healing which is known to be correlated with increased mitochondrial metabolism, NAD(P)H is furthermore the most important metabolic cofactor. In summary, NAD(P)H can be analysed both by fluorescence intensity detection and FLIM and therefore resembles the target molecule for non-invasive functional TPM [18].
We applied TPM to measure NAD(P)H related fluorescence intensities and lifetimes in order to detect cellular metabolic changes in corneal epithelial cells during wound healing in both a cell culture and an organ culture. Prior to the wound healing experiments our technical setup was tested and the method evaluated by alteration of the cellular microenvironment namely by changing temperature and by specific inhibition of cellular oxidative phosphorylation. In addition to fluorescence intensity we measured fluorescence lifetimes and calculated ratios of the contribution of a short and a long lifetime to the fluorescence decay. In terms of fluorescing NAD(P)H the two main species that are attributed to the two distinct lifetimes are its free and its protein-bound form. Free NAD(P)H features a lifetime between 200-500ps, whereas protein-bound NAD(P)H has a lifetime of 2000-3200ps [25].

	Intensity	**Fluorescence lifetimes**	**a1/a2 ratio**
Rotenone	↕	↓	↕
20°C	↓	↑	↓
42°C	→	↓	↑
Scratch	→	↓	↑
Erosion	→	↓	↑

Table 2: Change of fluorescence intensity, fluorescence lifetimes and free:protein-bound NAD(P)H ratio (a1/a2 ratio) within the different experimental groups.

The ratio of the contribution of free:protein-bound NAD(P)H to the fluorescence decay is a way to quantify metabolic shifts independent from overall NAD(P)H concentration and is therefore promising to be more sensitive to small changes than measuring fluorescence

intensity. In this study decrease of temperature and inhibition of oxidative phosphorylation by rotenone altered the cellular autofluorescence intensity significantly (Fig. 4) as demonstrated also by others in corneal keratocytes [14]. Rotenone prevents NAD(P)H from oxidation, hereby increasing overall NAD(P)H within mitochondria which hereby increases fluorescence intensity. However, following rotenone application glycolysis becomes upregulated in the cytoplasm as a metabolic compensation which is accompanied by decreased NAD(P)H binding to proteins and therefore decreases overall fluorescence lifetime [26]. In summary rotenone causes increased fluorescence intensity, decreased fluorescence lifetime and increased free:protein-bound ratio respectively (Fig. 4+5, Table 2).
Short term temperature reduction reduces metabolic activity within cells by reducing enzymatic activity globally [27]. Measurements at 20°C revealed a decrease in fluorescence intensity related to a decreased NAD(P)H concentration. Protein binding of NAD(P)H increased at low temperatures [28] and therefore were likely to cause increased lifetimes and reduced free:protein bound ratios (Fig. 4+5, Table 2).
In contrast, moderate temperature increases lead to optimal enzymatic function and enhanced cellular metabolism [27]. At 42°C fluorescence intensity did not change in comparison to the controls, however fluorescence lifetimes decreased significantly and free:protein-bound NAD(P)H ratios increased (Fig. 4+5, Table 2) indicating also enhanced glycolysis.
These experiments demonstrate that temperature induced increase in cellular metabolism does not change fluorescence intensity but fluorescence lifetimes and free:protein bound ratios.
In both wound healing experiments fluorescence intensities differed from the control groups, nevertheless none of the differences were statistically significant (Fig. 6+8) in contrast to fluorescence lifetimes and free:protein-bound ratios. Lifetimes decreased significantly following scratch or erosion. We interpret these decreased lifetimes following scratch or erosion as a shift from protein-bound NAD(P)H to free NAD(P)H caused by enhanced glycolysis as demonstrated above. The phase of glycolytic increase is then followed by a moderate decrease, depicted by increasing lifetimes over time until closure of the scratch/erosion. However these lifetime levels stay significantly below control lifetime levels in both experiments. As fluorescence intensities did not change significantly, we conclude that i: FLIM and calculation of free:protein-bound ratios are feasible to monitor metabolic changes during wound healing of corneal epithelial cells and ii: FLIM is a more sensitive method in this context than fluorescence intensity measurements.
As TPM is a non-invasive method it generally has the potential for *in vivo* applications in humans and has been established for imaging skin pathologies [29]. Our group has shown that, concerning the eye, TPM allows to detect immunological processes on a cellular level [30, 31], enabled for the first time a non-invasive quantification of corneal cross-linking effects based on fluorescence lifetime measurements (FLIM) [32] and detected interactions of immune cells and lymphatic vessels in real time [33].
The data presented now demonstrate the feasibility of TPM to analyze metabolic changes at the ocular surface during corneal epithelial wound healing by monitoring fluorescence lifetime changes. Besides technical improvements such as designing a suitable setup for *in vivo* imaging of human eyes the analysis of compartmentalized metabolic changes in cytosol, mitochondria and nucleus where metabolic cofactors function in different physiological processes will provide metabolic information on a single cell level as recently demonstrated in

C. trachomatis infected cells [17]. The future detection of cellular autofluorescence *in vivo*, in particular FLIM of metabolic cofactor NAD(P)H has the potential to become an inevitable tool in clinical use to differentiate healing from non-healing epithelial cells. This may support physicians in grading wound healing dysfunction in neurotrophic keratitis, limbus stem cell deficiencies or graft-vs.-host disease, etc. that all take place on a cellular and subcellular level. In addition TPM and FLIM may be used to measure and quantify immediate and long-term effects of different therapeutic strategies and also opens up possibilities to evaluate effects of newly developed substances on cellular metabolism in pre-clinical and clinical trials.

Acknowledgements

The authors would like to acknowledge Inke König, (Institute of Medical Biometry and Statistics, University of Luebeck) for substantial advice regarding statistical analysis and Daniela Rieck and Reinhard Schultz for superb technical support regarding tissue culturing and design of the custom made specimen holder. This study was supported by the University of Luebeck, Medical Faculty Grants (to PS).

References

1. **Nishida T, Chikama T, Morishige N, Yanai R, Yamada N, Saito J (2007) Persistent epithelial defects due to neurotrophic keratopathy treated with a substance p-derived peptide and insulin-like growth factor 1. Jpn J Ophthalmol 51: 442-447 DOI 10.1007/s10384-007-0480-z**
2. **Haruta Y, Ohashi Y, Matsuda S (1997) Corneal epithelial deficiency induced by the use of beta-blocker eye drops. Eur J Ophthalmol 7: 334-339**
3. **Dua HS, Saini JS, Azuara-Blanco A, Gupta P (2000) Limbal stem cell deficiency: concept, aetiology, clinical presentation, diagnosis and management. Indian J Ophthalmol 48: 83-92**
4. **Chen JJ, Tseng SC (1990) Corneal epithelial wound healing in partial limbal deficiency. Invest Ophthalmol Vis Sci 31: 1301-1314**
5. **Huttmann G, Lankenau E, Schulz-Wackerbarth C, Muller M, Steven P, Birngruber R (2009) [Optical coherence tomography: from retina imaging to intraoperative use - a review]. Klin Monbl Augenheilkd 226: 958-964 DOI 10.1055/s-0028-1109939**
6. **Erie JC, McLaren JW, Patel SV (2009) Confocal microscopy in ophthalmology. Am J Ophthalmol 148: 639-646 DOI S0002-9394(09)00457-7 [pii] 10.1016/j.ajo.2009.06.022**
7. **Radosevich AJ, Bouchard MB, Burgess SA, Chen BR, Hillman EM (2008) Hyperspectral in vivo two-photon microscopy of intrinsic contrast. Opt Lett 33: 2164-2166 DOI 172021 [pii]**
8. **Steven P, Müller, M., Koop, N., Rose, C., Hüttmann, G. (2009) Comparison of cornea module and DermaInspect noninvasive imaging of ocular surface pathologies. J Biomed Optics 14: 064040**
9. **Paulsen FP, Woon CW, Varoga D, Jansen A, Garreis F, Jager K, Amm M, Podolsky DK, Steven P, Barker NP, Sel S (2008) Intestinal trefoil factor/TFF3 promotes re-epithelialization of corneal wounds. J Biol Chem 283: 13418-13427 DOI M800177200 [pii]**

10.1074/jbc.M800177200

10. **Bird DK, Yan L, Vrotsos KM, Eliceiri KW, Vaughan EM, Keely PJ, White JG, Ramanujam N (2005) Metabolic mapping of MCF10A human breast cells via multiphoton fluorescence lifetime imaging of the coenzyme NADH. Cancer Res 65: 8766-8773 DOI 65/19/8766 [pii]**

10.1158/0008-5472.CAN-04-3922

11. **CHIA TH, WILLIAMSON, A., SPENCER, D.D., LEVENE, M.J (2008) Multiphoton fluorescence lifetime imaging of intrinsic fluorescence in human and rat brain tissue reveals spatically distinct NADH binding. Opt Express 16: 4237-4249**
12. **Kable EP, Kiemer AK (2005) Non-invasive live-cell measurement of changes in macrophage NAD(P)H by two-photon microscopy. Immunol Lett 96: 33-38 DOI S0165247803003341 [pii]**

10.1016/j.imlet.2003.12.013

13. **Li D, Zheng, W., Qu, J.Y. (2009) Two-photon autofluorescence microscopy of multicolor excitation. Opt Lett 34: 202-204**
14. **Piston DW, Masters BR, Webb WW (1995) Three-dimensionally resolved NAD(P)H cellular metabolic redox imaging of the in situ cornea with two-photon excitation laser scanning microscopy. J Microsc 178: 20-27**

15. Skala MC, Riching KM, Gendron-Fitzpatrick A, Eickhoff J, Eliceiri KW, White JG, Ramanujam N (2007) In vivo multiphoton microscopy of NADH and FAD redox states, fluorescence lifetimes, and cellular morphology in precancerous epithelia. Proc Natl Acad Sci U S A 104: 19494-19499 DOI 0708425104 [pii]
10.1073/pnas.0708425104
16. Vishwasrao HD, Heikal AA, Kasischke KA, Webb WW (2005) Conformational dependence of intracellular NADH on metabolic state revealed by associated fluorescence anisotropy. J Biol Chem 280: 25119-25126 DOI M502475200 [pii]
10.1074/jbc.M502475200
17. Szaszak M, Steven P, Shima K, Orzekowsky-Schroder R, Huttmann G, Konig IR, Solbach W, Rupp J (2011) Fluorescence lifetime imaging unravels C. trachomatis metabolism and its crosstalk with the host cell. PLoS Pathog 7: e1002108 DOI 10.1371/journal.ppat.1002108
PPATHOGENS-D-10-00626 [pii]
18. Huang S, Heikal AA, Webb WW (2002) Two-photon fluorescence spectroscopy and microscopy of NAD(P)H and flavoprotein. Biophys J 82: 2811-2825 DOI S0006-3495(02)75621-X [pii]
10.1016/S0006-3495(02)75621-X
19. Yu Q, Heikal AA (2009) Two-photon autofluorescence dynamics imaging reveals sensitivity of intracellular NADH concentration and conformation to cell physiology at the single-cell level. J Photochem Photobiol B 95: 46-57 DOI S1011-1344(08)00262-5 [pii]
10.1016/j.jphotobiol.2008.12.010
20. Lakowicz JR, Szmacinski H, Nowaczyk K, Johnson ML (1992) Fluorescence lifetime imaging of free and protein-bound NADH. Proc Natl Acad Sci U S A 89: 1271-1275
21. Anderson RA (1977) Actin filaments in normal and migrating corneal epithelial cells. Invest Ophthalmol Vis Sci 16: 161-166
22. Crosson CE, Klyce SD, Beuerman RW (1986) Epithelial wound closure in the rabbit cornea. A biphasic process. Invest Ophthalmol Vis Sci 27: 464-473
23. Kubawara T, Perkins, D.G., Cogan, D.G. (1976) Sliding of the epithelium in experimental corneal wounds. Invest Ophthalmol Vis Sci 15: 4-14
24. Rasband WS (1997-2011) ImageJ. U. S. National Institutes of Health, Bethesda, Maryland, USA.
25. Schneckenburger H, Wagner M, Weber P, Strauss WS, Sailer R (2004) Autofluorescence lifetime imaging of cultivated cells using a UV picosecond laser diode. J Fluoresc 14: 649-654
26. Erecinska M, Nelson D, Deas J, Silver IA (1996) Limitation of glycolysis by hexokinase in rat brain synaptosomes during intense ion pumping. Brain Res 726: 153-159 DOI 0006-8993(96)00324-1 [pii]
27. Sen S, Riaz SS, Ray DS (2008) Temperature dependence and temperature compensation of kinetics of chemical oscillations; Belousov-Zhabotinskii reaction, glycolysis and circadian rhythms. J Theor Biol 250: 103-112 DOI S0022-5193(07)00407-9 [pii]
10.1016/j.jtbi.2007.08.029
28. Somero GN (1975) Temperature as a selective factor in protein evolution: the adaptational strategy of "compromise". J Exp Zool 194: 175-188 DOI 10.1002/jez.1401940111
29. Konig K, Riemann I (2003) High-resolution multiphoton tomography of human skin with subcellular spatial resolution and picosecond time resolution. J Biomed Opt 8: 432-439 DOI 10.1117/1.1577349

30. Steven P, Rupp J, Huttmann G, Koop N, Lensing C, Laqua H, Gebert A (2008) Experimental induction and three-dimensional two-photon imaging of conjunctiva-associated lymphoid tissue. Invest Ophthalmol Vis Sci 49: 1512-1517 DOI 49/4/1512 [pii]
10.1167/iovs.07-0809
31. Gehlsen U, Huttmann G, Steven P (2010) Intravital multidimensional real-time imaging of the conjunctival immune system. Dev Ophthalmol 45: 40-48 DOI 000315018 [pii]
10.1159/000315018
32. Steven P, Hovakimyan M, Guthoff RF, Huttmann G, Stachs O (2010) Imaging corneal crosslinking by autofluorescence 2-photon microscopy, second harmonic generation, and fluorescence lifetime measurements. J Cataract Refract Surg 36: 2150-2159 DOI S0886-3350(10)01386-6 [pii]
10.1016/j.jcrs.2010.06.068
33. Steven P, Bock F, Hüttmann G, Cursiefen C (2011) Intravital Two-Photon Microscopy of Immune Cell Dynamics in Corneal Lymphatic Vessels. PLoS One 6(10) DOI 10.1371/journal.pone.0026253